Heat Treatment Study of Nb_3Sn strands for the Fermilab's High Field Dipole Model

E. Barzi, C. Boffo, P. J. Limon, J. P. Ozelis, R. Yamada, A. V. Zlobin
Fermi National Accelerator Laboratory, Batavia, IL, U.S.A.
E. Gregory, T. Pyon
IGC-AS, Waterbury, CT, U.S.A.
M. Wake
KEK, Japan

***Abstract*—Fermilab is developing high field superconducting dipole magnets based on Nb_3Sn for a post-LHC very large hadron collider (VLHC). The first prototype is a 1 meter long two-layer shell-type (cos-theta) coil with a nominal field of 11T. A keystoned Rutherford-type cable made of 28 Nb_3Sn strands of 1mm in diameter is used. The development of high J_c multi-filamentary Nb_3Sn strands with low magnetization is an important step of this program. To achieve this goal, strand R&D is actively pursued by Fermilab and IGC using the internal tin process. Conductor designs, heat treatment studies, and results of measurements, including I_c, n-value, RRR, magnetization, and chemical analyses, are presented.**

I. INTRODUCTION

Within the framework of an R&D program towards a post-LHC very large hadron collider (VLHC), a high field Nb_3Sn dipole magnet (HFM) with a nominal field of 10-11T is being developed at Fermilab.[1] The maximum field, B_{max}, is determined by the coil width and by the critical current density, J_c, of the superconductor. On the other hand, the field uniformity in the bore is very sensitive to superconductor magnetization, which is proportional to the effective filament diameter, d_{eff}, of a multifilamentary strand. Hence, for a cost effective and reliable magnet design, J_c should be as high, and d_{eff} as low as possible. Multifilamentary Nb_3Sn is one of the most promising materials to achieve these goals. Strand R&D is actively pursued by Fermilab and IGC using the internal tin process and, as a benchmark, the strand design developed for ITER.[2]

The J_c of a Nb_3Sn strand depends on several factors. In the internal tin process, these factors include: number and design of the strand subelements, amount of tin and of niobium in the non-copper section, type of niobium alloy used, copper to non-copper ratio, and the heat treatment cycle given to the wire. This paper addresses such J_c sensitivity issues, with a special focus on heat treatment effects. Three heat treatment cycles, differing in the temperature of their last step, were applied to two Nb_3Sn strands of different designs (named T and C) produced by IGC. The effects on J_c, n-value, RRR, and magnetization are presented, as well as a measure of Sn diffusion in the strand cross section. This was done performing a point to point compositional analysis of the Cu-Sn matrix and of the Nb-Sn filaments by Energy Dispersion X-rays Spectroscopy (EDS).

II. R&D STRAND DESCRIPTION

A. Strand parameters

The geometrical parameters of the IGC superconducting Nb_3Sn strands that were used for this study are summarized in Table 1.

TABLE 1. Nb_3Sn STRAND PARAMETERS

Parameter	Strand T	Strand C
Strand diameter, mm	1.000±0.002	0.999±0.002
Number of subelements	61	37
Cu to non-Cu ratio	0.87:1	0.87:1
RRR	> 300	> 300
Sn content	Intermediate	Intermediate-high
Nb-alloy	Type A	Type B
Nb filament diameter, μm	4.1	5.3

An *intermediate* Sn amount corresponds to a Sn content in the non-Cu section of a strand ranging from 13 to 15 at.%.

Given the same copper to non-copper ratio of strands T and C, any comparison in J_c performance between these strands can be made using the critical current, I_c.

B. Strand preparation and measurements procedure

For this study, three sets of samples were prepared and tested. A different thermal cycle was used for each set to monitor the dependence of the strand superconducting properties on heat treatment. Set 1 included 2 samples from strand C, and 7 from strand T. The strand T samples came from a different restack of the same original billet, whereas the 2 samples from strand C belonged to the same restack. Set 2 comprised 2 samples from strand C, and 6 from different restacks of strand T. Set 3 included 2 samples from strand C, and 2 samples from two different restacks of strand T. All sets also included specimens to measure the strand magnetization. The samples to be used for I_c measurements were wound on grooved cylindrical barrels made of Ti-6Al-4V alloy, and held in place by two removable Ti-alloy end rings.[3] Those to be used in magnetization measurements were wound on stainless steel tubes. All sets were heat treated in an argon atmosphere according to the schedules given in Table 2 for HT-1, HT-2, and HT-3 respectively. For HT-3, the 17 hours at 750°C were I_c optimized within a couple of hours range.

Manuscript received September 27, 1999.
This work was supported by the U. S. Department of Energy.

TABLE 2. HEAT TREATMENT CYCLES

Heat treatment		Step 1	Step 2
Ramp rate, °C/h		25	25
Temperature, °C	**HT-1**	575	**650**
Duration, h		200	180
Ramp rate, °C/h		25	25
Temperature, °C	**HT-2**	575	**700**
Duration, h		200	90
Ramp rate, °C/h		25	25
Temperature, °C	**HT-3**	575	**750**
Duration, h		200	17

After the reaction phase, the Ti-alloy end rings of the cylindrical barrels were replaced by Cu rings, and voltage-current characteristics were measured in boiling He at 4.2 K, in a transverse magnetic field from 10 T to 15 T. The relative directions of external magnetic field and transport current were chosen such as to generate an inward Lorentz force. By considering also the differential thermal contraction between the sample and the Ti-alloy barrel, this causes the Nb_3Sn composite to be subject to a tensile strain of up to +0.05% at 12 T[4], which leads to a systematic error in the 3-5% range on I_c.

Voltages were measured along the sample by means of voltage taps placed 50 cm apart. The I_c was determined from the voltage-current curve using the 10^{-14} Ω·m resistivity criterion. By fitting this curve with the power law $V \sim I^n$, n-values were determined in the voltage range from V_c to $10 \cdot V_c$ at a given magnetic field, where V_c is the voltage corresponding to I_c. The estimated uncertainty of the I_c measurements is less than ± 2%, and it is about ± 12% for the n-values.

The specimens wound on the stainless steel tubes were removed and slid on a G10 holder. Magnetization measurements were performed by means of a balanced coil magnetometer. The estimated uncertainty of the AC losses measurements is ± 1.5% for 0-3 T loops, and ± 2.5% for 10-13 T loops.

Figure 1. Cross section of an IGC Nb_3Sn wire with a copper to non-copper ratio of 0.65:1.

The Cu to non-Cu ratio is measured using an image analysis software. The validity of this method was checked for the strand shown in Figure 1, whose Cu to non-Cu ratio had been measured by etching. The digital method gave 0.646, whereas the etching method produced a value between 0.64 and 0.65.

III. TEST RESULTS AND DISCUSSION

A. *Critical current, n-value, and RRR*

The I_c results are shown in Figures 2 and 3 as a function of magnetic field. For strand T, the I_c's are averaged over all the T samples of each set. Similarly, in Figures 4 and 5 the n-values are shown. One can see that for both strands T and C, HT-3 is obviously the worst heat treatment with respect to I_c, but that HT-1 becomes relevantly better than HT-2 only below 13.5T for strand T, and below 15 T for strand C. Moreover, while the n-values for strand C show a very weak sensitivity to heat treatment, for strand T they are highest over the whole field range of interest with HT-2. This could be due to an optimization of time and temperature to enhance the homogenization of Nb filament reaction.

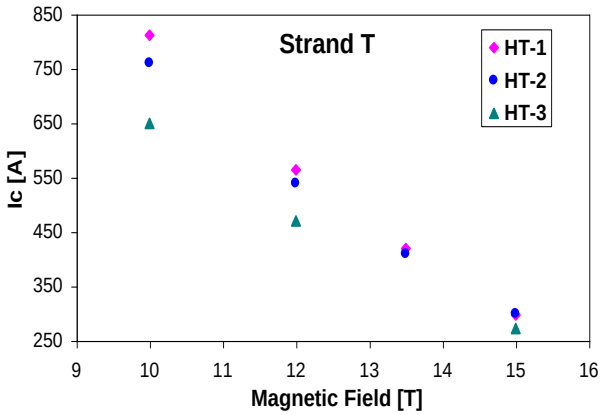

Figure 2. I_c dependence on field for strand T.

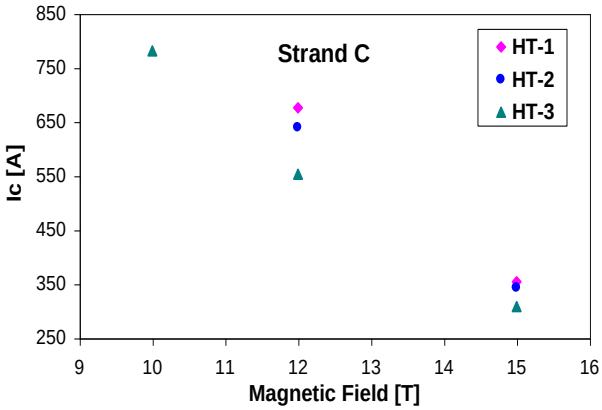

Figure 3. I_c dependence on field for strand C.

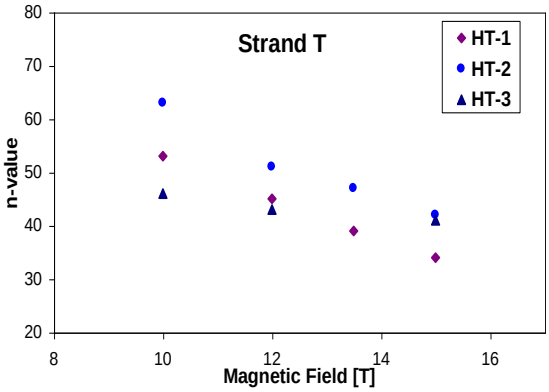

Figure 4. n-value dependence on field for strand T.

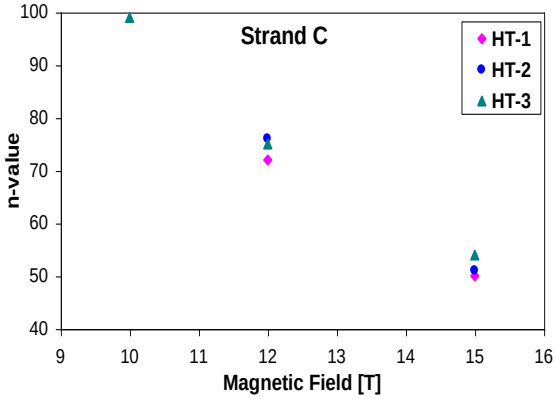

Figure 5. n-value dependence on field for strand C.

However, this same combination of time and temperature (*i.e.* HT-2) appears to produce the lowest RRR, as can been observed from Figure 6, although errors are large. If the diffusion barrier is broken, HT-2 would allow a larger contamination of the Cu by the Sn. The generally low RRR's in Figure 6 may account for broken barriers with any heat treatment, as also Figure 12 suggests. This is a field emission SEM picture of strand T after HT-1, and barrier breakages can be seen in at least three points adjacent to copper channels of the split sub-elements. Barrier breakages may arise from the lack of lower temperature steps in the heat treatments.

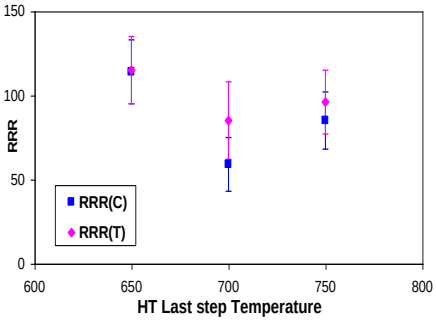

Figure 6. RRR dependence on thermal cycle.

In Figures 7 and 8, the I_c and n-value dependence on heat treatment are shown at various magnetic fields for both strands C and T. At 12T, the I_c and n-value of strand C versus strand T are better by 18-20% and 50-75% respectively.

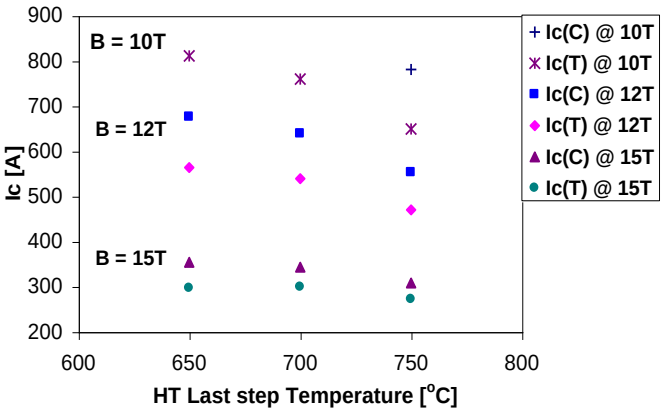

Figure 7. I_c dependence on thermal cycle.

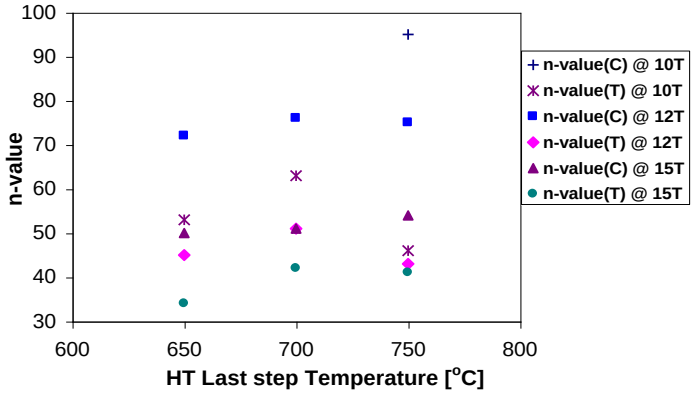

Figure 8. n-value dependence on thermal cycle.

In Figure 9, the dependence on heat treatment of the I_c normalized to I_c from HT-1 is plotted at 12T for strands C and T. One can see that within the measurement uncertainties, the same scale factors can be applied to the I_c's of both strands. This is true also for the n-values.

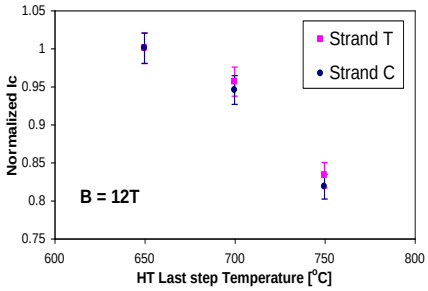

Figure 9. Normalized I_c dependence on thermal cycle.

B. AC losses and d_{eff}

In Figure 10, the AC losses for a 0-3T loop at 1T/min., and d_{eff} at 12T are shown for both strands C and T as a function of heat treatment. One can see that d_{eff} increases with temperature. This was predictable by d_{eff} being inversely proportional to I_c, since at 12T I_c decreases with temperature, as Figures 7 and 9 show.

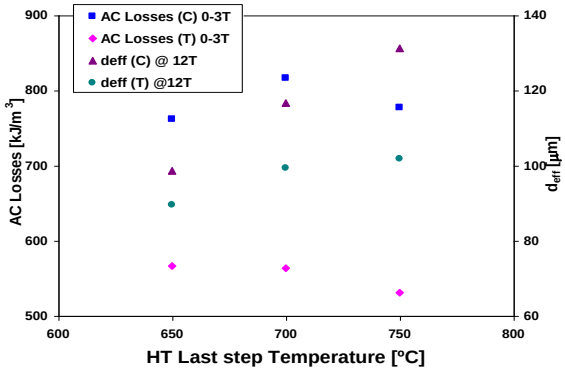

Figure 10. AC losses and d_{eff} dependence on thermal cycle.

The magnetization hysteresis curves of type A and type B Nb rods were also measured to investigate the alloy quality. They are plotted in Figure 11. As can be seen, their lower and upper critical fields at 4.2K, shown in Table 3, are very similar. Then only the higher Sn content in the non-Cu section is left to explain the better I_c performance of strand C.

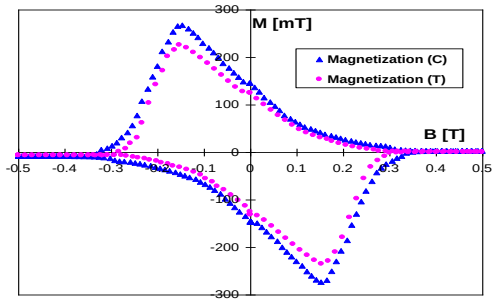

Figure 11. Magnetization loops of type A and B Nb-alloys.

TABLE 3. Nb-ALLOYS CRITICAL FIELDS AT 4.2K

Nb-alloy	H_{c1} [mT]	H_{c2} [mT]
Type A	182	316
Type B	181	341

C. *Chemical analysis*

Finally, a measure of Sn diffusion in the strand cross section was made by performing a compositional analysis of the Cu-Sn matrix and of the Nb-Sn filaments by EDS in all points shown in Figure 12. The results are given in Table 4. The errors on the Sn and on the Nb concentrations are less than 10% and 2% respectively.

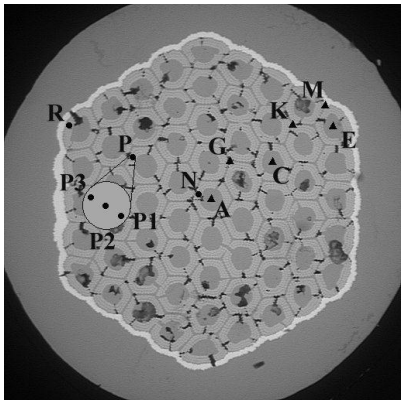

Figure 12. Field emission SEM picture of strand cross sections. The letters indicate the points where the analysis was made.

These data show a high uniformity of Sn concentration both in the matrix and in the filaments. They do not prove any correlation of Sn diffusion with the I_c's produced by the three heat treatments, neither in the matrix nor in the filaments. However, one may find an indication of a decrease in I_c with a Sn depleted bronze and possibly overreacted filaments. As shown by the EDS analysis, the Nb filaments underwent a complete reaction even in the case of the thermal cycle giving the poorest performance, *i.e.* HT-3. This is consistent with the fact that the time to hold at 750°C (*i.e.* 17 hr.) had been I_c optimized. The strand diameter dependence on heat treatment, measured as a possible indication of superconducting layer growth, and shown in Figure 13 for strand C, would account only for a very small difference in the increase of cross sectional areas. Therefore, what determines the lower I_c's in the higher temperature thermal cycles must be a J_c reduction, probably due to the decrease of pinning center density due to excessive grain growth, and the consequent decrease of the grain boundary surface.

TABLE 4. COMPOSITION OF THE Cu-Sn MATRIX AND OF THE Nb-Sn FILAMENTS AFTER EACH HEAT TREATMENT

Position	Sn [atm.%] – Cu-Sn MATRIX		
	HT-1	HT-2	HT-3
A	4.8	4.9	4.2
G	5.1	4.3	4.4
C	4.7	4.1	3.9
K	5.6	5.0	4.2
E	5.0	4.1	4.2
M	4.6	3.8	4.5
Weighted average	4.95 ± 0.20	4.42 ± 0.16	4.23 ± 0.11
Rms	0.36	0.48	0.21
	Nb [atm.%] – Nb-Sn FILAMENTS		
N	74.2	74.2	73.3
P	75.3	75.4	73.4
R	75.5	73.5	75.1
Weighted average	75 ± 0.69	74.41 ± 0.77	73.89 ± 0.50
Rms	0.70	0.96	1.01

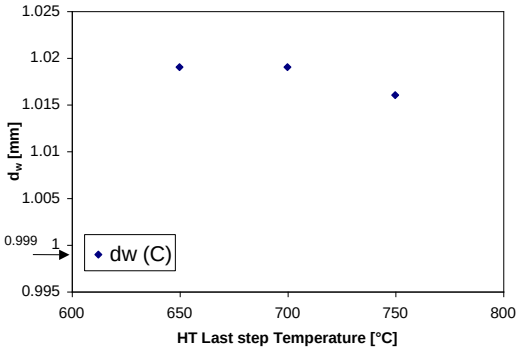

Figure 13. Diameter dependence on thermal cycle for strand C. The arrow indicates strand C diameter before heat treatment.

IV. SUMMARY

The present study of heat treatment effects on I_c and d_{eff} was performed for two types of internal tin Nb_3Sn strands. It was found that the lowest temperature cycle provided the highest I_c and the lowest d_{eff} values. However, both these parameters still need improvement in order to meet Fermilab's strand specifications for high field accelerator magnets.

REFERENCES

[1] G. Ambrosio et al., "Conceptual Design of the Fermilab Nb_3Sn High Field Dipole Model", PAC'99, New York, NY, USA, March 1999.

[2] E. Gregory et al., "Properties of internal tin Nb_3Sn strand for the International Thermonuclear Experimental Reactor", Advances in Cryogenic Engineering, Vol. 42, Plenum Press, New York, 1996.

[3] L. F. Goodrich et al., "Superconductor critical current standards for fusion applications", NISTIR 5027, NIST.

[4] E. Barzi et al., "Error analysis of short sample J_c measurements at the Short Sample Test Facility", Fermilab, TD-98-055, Sept. 1998.